



# Correlating dry wear turning and pin-on-disc tests: a cost-effective approach to machinability evaluation for low carbon steel grades

Daniel Martínez Krahmer<sup>1,3</sup> · Vitaliy Martynenko<sup>1,2</sup> · Alberto Pereyra Osenda<sup>3</sup> · Antonio J. Sánchez Egea<sup>4</sup> 

Received: 19 June 2023 / Accepted: 23 October 2023  
© The Author(s) 2023

## Abstract

Machinability tests play a crucial role in the metalworking industry despite their inherent cost and time requirements. This study aims to introduce a novel approach by establishing a correlation between the dry wear turning and pin-on-disc tests, potentially enabling their interchangeability. The industry is particularly interested in this challenge due to the simplified implementation and reduced costs and time compared to the conventional turning test. The correlation between the dry wear turning and pin-on-disc tests was investigated using three low carbon steel grades (12L14, 1212, and 1018) and three medium cutting speeds (150, 180, and 240 m/min). Additionally, a comprehensive cost-energy comparison is conducted to underscore the significance of identifying a laboratory test equivalent to the traditional machinability test. The obtained results reveal a strong correlation between both wear tests. Furthermore, the relative cost analysis demonstrates that the pin-on-disc test costs only 14% of the long-duration turning test, emphasizing its cost-effectiveness.

**Keywords** Machinability · Pin-on-disc · Abrasiveness · Wear · Steels

## 1 Introduction

Machining processes are extensively utilized in the metal processing sector for part manufacturing [1]. In response to global efforts to reduce environmental impact and protect operator health, there has been a significant push to minimize or eliminate the use of cutting fluids. As a result, substantial research efforts have focused on the development

and implementation of dry machining. This research encompasses various aspects, including the optimization of machining operations, the selection of materials, and the utilization of appropriate tools [2]. Steel alloys are a predominant material group subjected to machining operations, constituting a substantial proportion of the sector's output. Within the realm of steel alloys, low carbon steels [3] and Free-Cutting Steels (FCS) [4] have gained prominence for manufacturing parts with minimal mechanical compromises. Notably, FCS stand out by offering superior machinability, enhanced finishing quality, and effective chip control [5].

Machinability tests establish a relationship between the behavior during the machining of a material against a given tool. The evaluation of flank wear ( $V_B$ ) serves as the primary criterion for this assessment. Typically, this type of wear prevails along the cutting edges of the tools [6]. However, tests designed to determine long-term tool life demand substantial time and significant material quantities for machining [7], rendering them both costly and challenging to execute. To mitigate these drawbacks, alternative testing methods, such as short-term tool life tests, have been explored [8]. These tests involve a combination of a facing operation utilizing a high-speed steel tool and an elevated cutting speed intentionally chosen to cause the tool to lose its cutting effectiveness within a single pass [9]. Nevertheless, this approach may

---

Technical Editor: Diego Carou Porto.

✉ Antonio J. Sánchez Egea  
antonio.egea@upc.edu

<sup>1</sup> Centro de Investigación y Desarrollo en Mecánica, Instituto Nacional de Tecnología Industrial, INTI, Avenida General Paz 5445, 1650 Miguelete, Provincia de Buenos Aires, Argentina

<sup>2</sup> Facultad de Ingeniería, Universidad Nacional de Lomas de Zamora, Camino de Cintura y Juan XXIII, Lomas de Zamora, Provincia de Buenos Aires, Argentina

<sup>3</sup> Instituto de Tecnología E Ingeniería, Universidad Nacional de Hurlingham, Av. Gdor. Vergara 2222, Villa Tesei, Provincia de Buenos Aires, Argentina

<sup>4</sup> Department of Mechanical Engineering, Universitat Politècnica de Catalunya, Av. de Víctor Balaguer, 1, 08800 Vilanova I La Geltrú, Barcelona, Spain

not represent the most optimal technical choice when compared to the long-term tool life-turning tests, primarily due to its reliance on high-speed steel tools, which are not commonly employed within the industry. An alternative option emerges from the method initially proposed by Stahl and Andersson [10]. They defined the machinability of a material as a function of five variables: hardness, abrasiveness, thermal conductivity, ductility and strain hardening. After establishing these parameters, they coalesce to create a polar machinability diagram characterized by a pentagonal shape. This diagram functions as a tool for classifying materials that exhibit similar diagrams, indicating shared machining characteristics. The significance of each variable's contribution varies depending on the material type. For instance, in stainless steels, the dominant factors are ductility, thermal conductivity, and strain hardening, whereas in low to medium carbon steels, hardness and abrasiveness exert the primary influence [11].

Considering that abrasive wear is typically observed when a hard material interacts with a softer material, like low carbon steel [12], we suggest establishing a correlation between the conventional machinability test acquired through dry turning and the abrasiveness determined via pin-on-disc tests. In this setup, a carbide pin simulates a cutting tool, while varying grades of steel discs serve as the workpieces. Two types of tests are carried out on low carbon steel grade AISI 1018 and FCS grades AISI 1212 and AISI 12L14. Avdovic et al. [13] introduced the polar machinability diagram to different Inconel 718 batches and defined the abrasiveness directly with carbon percentage. In this work, since the three steel grades under study are similar (they present nominal carbon percentages between 0.10 to 0.18%), we consider the possibility of evaluating the abrasiveness by the pin-on-disc method. Therefore, the novelty of this work is to establish a correlation between a turning test and a pin-on-disc test to show their possible interchangeability. This novelty may be of considerable industrial interest due to the simplicity of implementing pin-on-disc tests and their reduced cost energy compared to a traditional machinability test.

## 2 Materials and methods

### 2.1 Machining test

Drawn bars of three different steel grades, AISI 1018, AISI 1212 and AISI 12L14, were studied in this research. The as-received geometrical dimensions were 38.1 mm in diameter and 350 mm in length. The machinability tests were performed in a CNC lathe (Promecor SMT 19/500, Cordoba, Argentina), where the conditions of the round-turning process for each steel grade were the same as in

our previous works [14, 15]. Cutting tools with uncoated inserts (type CNMG120408 and quality ISO P40, Kennametal, Latrobe, USA) and specific tool-holder (type MCLNR-2525M12, Kennametal, Latrobe, USA) was the configuration for the machining experiments. The finishing cutting conditions used in this work were a depth of cut 1.25 mm, feed rate of 0.125 mm/rev and three cutting speeds ( $V_c$ ) 150, 180 and 240 m/min, as fabricant Kennametal recommends for these types of steel [16]. The wear evolution at the cutting edge ( $V_B$ ) was determined using an optical measuring benchmark (Dormer, Model 94, England). Following the standard ISO 3685 [7] that established the criterion of interruption test, given the reduced wear resistance of the ISO P40 quality inserts, the wear stop criterion was set at  $V_B = 0.5$  mm for these steel grades due to the fast wear rate found during preliminary experiments. Since the wear rate of the pin-on-disc test is measured in  $\text{mm}^3/\text{min}$ , a rate with the equivalent unit in the machinability test is desired. Accordingly, the wear volume insert is determined when reaching  $V_B = 0.5$  mm. Thus, Fig. 1 shows the geometrical relationship to determine this wear during machining.

$$\tan \alpha = \frac{x}{V_B} \rightarrow x = V_B \tan \alpha$$

$$\text{Triangle area} = \frac{V_B x}{2} = \frac{V_B^2 \tan \alpha}{2}$$

$$\text{Equivalent wear volume} = \text{Triangle area} * l = \frac{p}{\cos \theta} \frac{V_B^2}{2} \tan \alpha = 0.014 \text{ mm}^3$$

where  $X$  is the horizontal wear on the insert cutting edge (mm),  $V_B$  is the flank or vertical wear on the side relief face of the tool (stop criterion at 0.5 mm),  $\alpha$  is the angle of the side relief face of the insert ( $5^\circ$ ),  $p$  is the depth of cut (1.25 mm),  $\theta$  is the angle of the main cutting edge ( $5^\circ$ ) and  $l$  is the contact length between tool cutting edge and work-piece (mm). Figure 2 shows the two technologies, machining and pin-on-disc, which are used to study the machinability of steels.

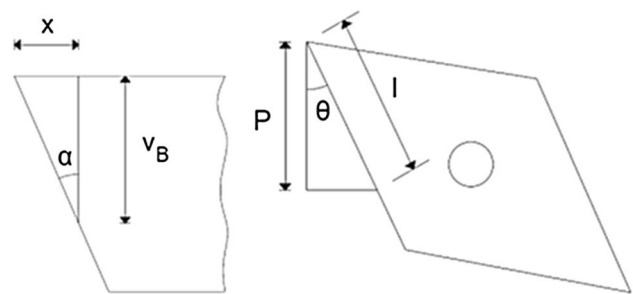


Fig. 1 Equivalence between flank wear and worn edge volume

## 2.2 Pin-on-discs test

Six discs were made of each steel grade, AISI 1018, AISI 1212 and AISI 12L14, from drawn bars of 50 mm diameter to be tested in the in-house pin-on-disc machine. During these tests, 36 carbide pins (ISO K20-K40 / P20-P40) were made from hard metal bars with a nominal diameter of 6.35 mm. The ends of the bars were ground into a hemispherical shape with a radius of 2 mm with a plane of 0.25 mm in diameter. Both faces of the discs were grounded on a tangential grinding (Davonis SGS-1230AHR, Buenos Aires, Argentina), using an A46I10V grinding wheel with an average grain size of 0.38 mm. During the pin-on-disc tests, three different tangential contact velocities were applied 150, 180 and 240 m/min (same velocities as the machining tests) in the three steel grades and four repetitions to ensure the repeatability of the tests. In total, 36 pin-on-disc tests were done. A cleaning procedure of 15 min of ultrasonic bath (J.P. Selecta S.A., model: 3,000,683) with isopropanol was applied to each sample before measuring the weight loss. The weight difference to determine the abrasiveness was

recorded with a Radwag electronic scale, model AS 220. R2 (Radwag, Radom, Poland), with an accuracy of 0.1 mg. Finally, the pin-on-disc tests were performed at  $21 \pm 3$  °C and a relative humidity of  $50 \pm 10\%$ .

## 2.3 Metallographic analysis

An energy-dispersive X-ray spectroscopy module (UTW-Sapphire, model: PV7760/79 ME) was used to investigate the presence of chemical elements on hard metal pins, as shown in Table 1. Table 2 shows the chemical composition of the discs performed by optical emission spark spectroscopy (OES-spark). The determinations were carried out with a Bruker spectrometer, model Q4 Tasman following the guidelines of ASTM E415:17 Standard Test Method for Analysis of Carbon and Low-Alloy Steel by Atomic Emission Spectrometry. Regarding the hardness measurements, a hardness tester (Digimesh MHVD-10000AP, China) was used to measure the hardness of the discs and pins with a load of 100 g for 10 s. Finally, an SEM microscope (FEI

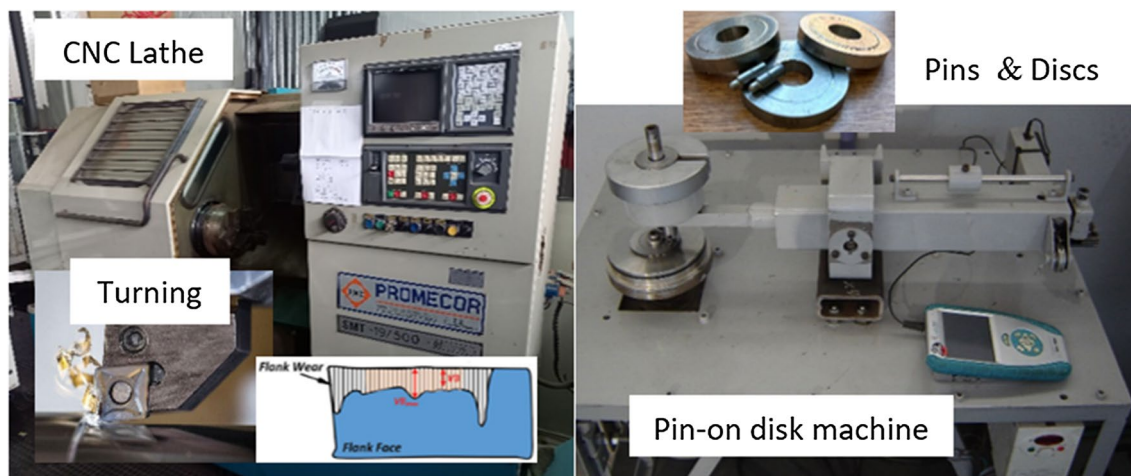


Fig. 2 Schematic of the machines and tools used to perform the wear experiments

**Table 1** Chemical composition and hardness of carbide pins

Hard metal quality	Chemical composition (wt%)			Vickers hardness HV 0.1
	W	C	Co	
ISO K20-K40/P20-P40	$75.00 \pm 1.02$	$18.30 \pm 2.14$	$6.84 \pm 2.07$	$1700 \pm 190$

**Table 2** Chemical composition, hardness and grain size of the discs

Steel of disc	Chemical composition (wt%)						HV 0.1	Grain size (um)
	C	Mn	S	P	Pb	Fe		
AISI 1018	0.247	0.686	0.023	0.021	0	Balance	$181.7 \pm 23.6$	G 6.5
AISI 1212	0.069	1.361	0.389	0.037	0	Balance	$170.7 \pm 20.7$	G 7.5
AISI 12L14	0.079	1.964	1.395	0.035	>0.3	Balance	$177.7 \pm 16.4$	G 8.0

QUANTA 250 FEG) was utilized to determine the main wear parameters.

The sample inclusions were made using a self-curing acrylic polymer and a pressure chamber, model Allied 175–10,000, with a capacity of up to 30 psi. Later, the metallographic specimens were polished to 1200 silicon carbide paper and then with cloth and 0.3  $\mu\text{m}$  alumina in a Struers 05426327 polishing machine (Denmark). The microstructure was developed in all cases with Nital 4% reagent by bath for 10 s. Finally, the metallographic specimens were prepared following the procedure indicated in ASTM Guide E3 to determine the geometry of the wear tracks and the plastically deformed zone. Also, grain size determination was carried out according to ASTM E112-13.

### 3 Results and discussion

#### 3.1 Machining test

The conventional machinability was measured by turning operations on the three steel grades at 150, 180 and 240 m/min cutting speeds, as recommended by Kennametal [16]. Figure 3 shows the Taylor lines for each steel grade.

Taylor lines represent the tool life of the cutting edge as a function of cutting speed and machined material. Table 3

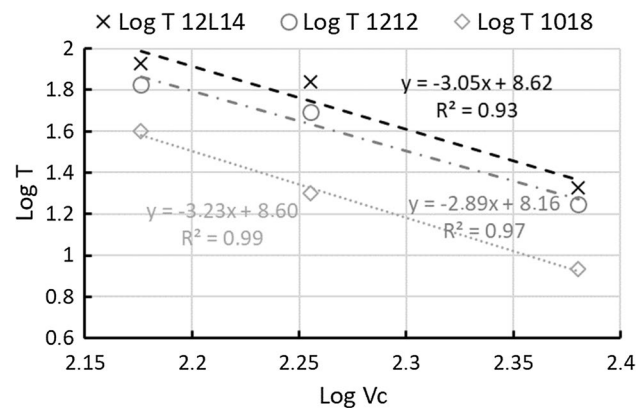


**Fig. 3** Taylor lines were obtained during the machining of the three steel grades

**Table 3** Machinability test results

Steel grade	Stop criterion VB (mm)/equivalent wear volume ( $\text{mm}^3$ )	Tool life at 150 m/min (min)	Tool life at 180 m/min (min)	Tool life at 240 m/min (min)
AISI 1018	0.5/0.014	39.76	19.90	8.60
AISI 1212		66.80	49.30	17.68
AISI 12L14		84.40	69.17	21.15

exhibits the machinability test results at 150, 180 and 240 m/min and the time to reach the stop criterion of wear on the side relief face of the cutting tool. The results show similar trends with an offset between the materials. When cutting AISI 1018 steel, the tool life was significantly lower than the other two steel grades. The improvements achieved in the performance of the free-cutting steels are obtained from the addition of lead and manganese sulphide [17]. It is denoted that the average tool life when cutting AISI 1018 is at least 43.4% smaller than the FCS, similar results are found in [16].

#### 3.2 Pin-on-discs test

The duration of the pin-on-disc tests was 90, 70 and 20 min for the cutting speed of 150 m/min, 180 m/min and 240 m/min, respectively (see Table 3, maximum tool life at each cutting speed). These durations are usual lifetimes on free-cutting steels with this type of tool and cutting conditions. The load applied was experimentally determined from previous studies [5], resulting in an average contact pressure in the range of 335 (initial stage) to about 165 MPa (final stage). However, we consider using the contact pressure at the final stage because the contact pressure at the initial stage is not very representative, given the rapid settling of the cutting edge. Thus, the contact pressure used is the result of having 50 N of feed force divided per the 1.25 mm of pass depth and 0.3 mm of flank wear. This contact pressure for the pin with a 0.25 mm diameter flat at the tool tip represents a load of 8.5 N. Additionally, the friction coefficient is calculated as the ratio between the average tangential force obtained during the last 5 min of the test and the load on the pin at a speed of 150 m/min. The friction coefficient is calculated as the ratio between the average tangential force obtained during the last 5 min of the test and the load on the pin at a speed of 150 m/min. The tangential force was recorded with a Vernier model LabQuest data logger with a load range of up to 50 N, while the contact temperature was measured with a Flir E60 thermographic camera. The results showed a friction coefficient of  $0.470 \pm 0.032$  for a temperature of  $63.0 \pm 2.6$   $^{\circ}\text{C}$  for AISI 1018; a friction coefficient of  $0.439 \pm 0.002$  for a temperature of  $55.3 \pm 2.5$   $^{\circ}\text{C}$  for AISI 1212 and a friction coefficient of  $0.485 \pm 0.017$  for



a temperature of  $64.3 \pm 3.2$  °C for AISI 12L14. Therefore, there were no significant differences between the measured values, but a certain correlation between friction coefficient and temperature was observed. Also, Table 4 shows the weight loss and wear rate of each steel grade pin-on-disc tested at 150, 180 and 240 m/min.

As cutting speed increases from 150 m/min to 240 m/min, the weight loss decreases for all steel grades (AISI 1018, AISI 1212, and AISI 12L14). This suggests that higher cutting speeds result in more efficient machining processes, reducing the amount of material worn away per minute and overall weight loss. Additionally, among the steel grades, AISI 12L14 consistently exhibits the highest wear rates, while AISI 1018 generally has the lowest wear rates. The presence of lead in AISI 12L14 contributes to its higher wear rate, while AISI 1018 exhibits lower wear due to its wear-resistant properties. These correlations emphasize the significant influence of cutting speed and steel grade on disc wear in pin-on-disc tests.

## 4 Metallography

SEM microscope is used to observe possible material adhesion in the surface of the carbide pins, revealing a minimum material adhesion was found. However, the electron microscope revealed two things: 1) the existence of an ellipse-shaped, completely worn elliptical area, and 2) a little material adhering to part of the perimeter of this area, see Fig. 4. Note that pins in their original state had circular and concentric machining marks (see Fig. 4a). These marks have entirely disappeared in the worn area. Also, this disproportion is due to the asymmetry hardness of pins (1700 HV) and discs (150–205 HV). Also, the steel grades are ordered from highest to lowest degree of pin wear, AISI 1018, AISI 1212 and AISI 12L14, similar to the previously reported [18]. The elliptical worn areas would indicate an order equal

to that obtained in long time tool life turning machinability tests with wear areas of 915, 860 and 615  $\mu\text{m}^2$ , respectively. Microscopic images of the wear tracks at the discs exhibit pearlite oriented in long vertical black lines and ferrite as balance, except in the deformation zone where the pearlite is agglomerated.

The adhesion phenomenon on the cutting tool edge, known as Built Up Edge (BUE), was not observed in long-time tool life turning tests on different steels and at any of the cutting speeds tested. It commonly occurs in machining medium to low carbon steels using uncoated inserts when cutting velocities of at least 125 m/min are used [12]. Figure 5 shows a schematic of wear tracks and the variables to characterize the wear profile.

Table 5 shows geometric values measured in wear tracks of each steel grade, where W represents the distance between burr peaks, h is the depth of the wear track, w is the width of the wear track without burrs, p1 is the height of the internal burr (near the lowest tangential velocity) and p2 is the height of the external burr (near the highest tangential velocity). Note that depth is the thickness of the plastically deformed zone. Since the cross sections of wear tracks for AISI 1212 and 12L14 steel are similar in both width (w) and depth (h), but AISI 12L14 steel discs experienced more significant weight loss (see Table 4), the difference can be explained by the size of burrs, significantly larger in case of AISI 1212, and present around the entire perimeter of the track, both inside and outside. Likewise, material hardness was measured in this plastically deformed zone, differentiating three different zones, the inner one (zone of lower tangential velocity), the central one (where pin axis contacts bottom of wear track) and the outer one (zone of higher tangential velocity). Concerning the plastically deformed zone, while AISI 12L14 steel disc has 82.4  $\mu\text{m}$ , AISI 1018 was 124.2  $\mu\text{m}$  and AISI 1212 was 131.4  $\mu\text{m}$ .

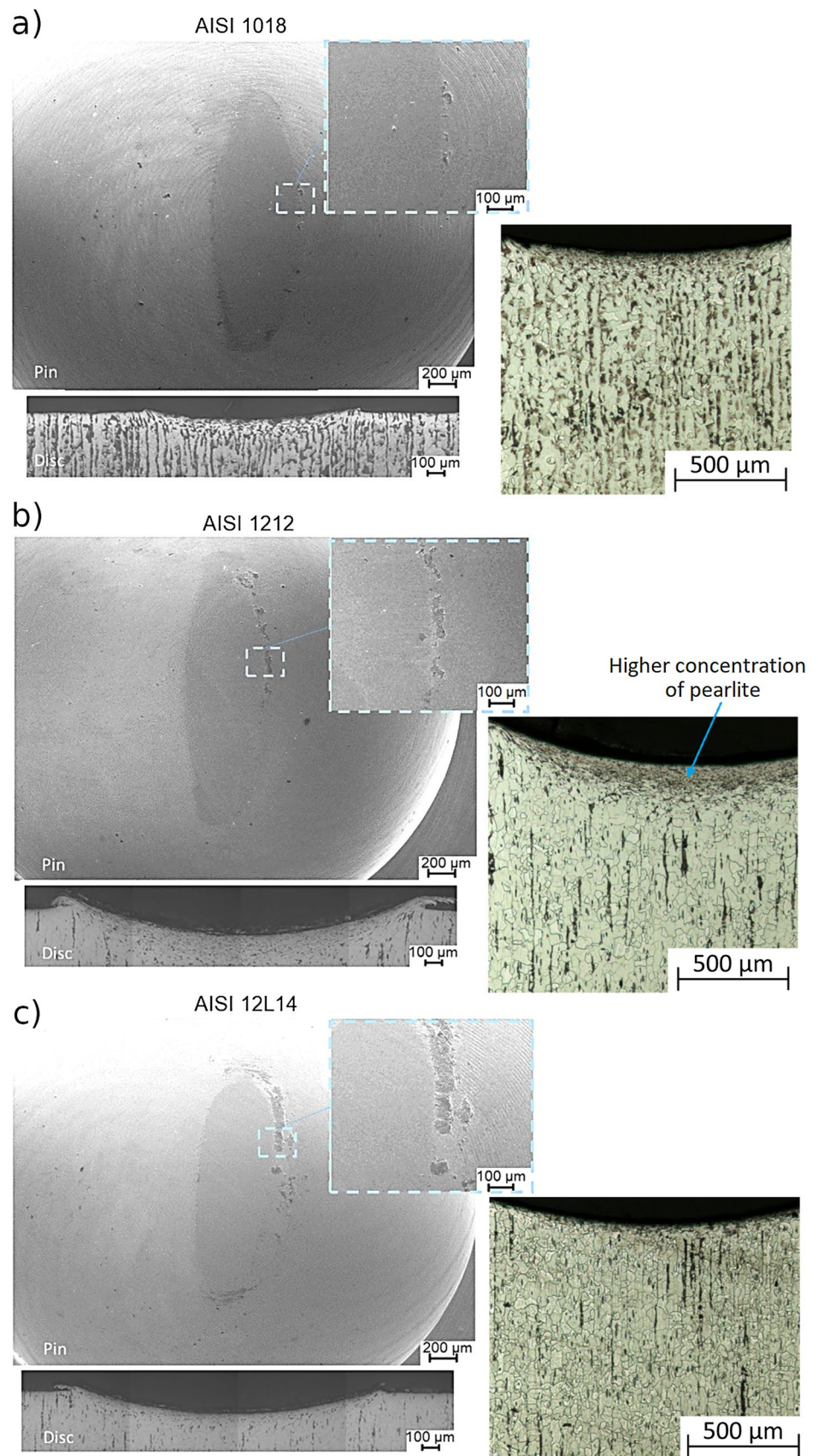
Figure 6 displays the material hardness values for the three steel grades at different measurement points (initial, internal burr, centre, and external burr) along with their respective standard deviations.

The result suggests that steel grade significantly influences material hardness, with 1212 steel generally exhibiting the highest hardness values across different locations. 1018 steel demonstrates higher hardness, particularly in the initial state. Meanwhile, 12L14 steel tends to have lower hardness values but displays less variability, as indicated by its smaller SD values. Relating these hardness values to metallography (see Fig. 4), it is denoted that the deformed zone of AISI 1212 grain size is significantly smaller and has a higher density of pearlite (see Fig. 4b). This microstructure characteristic justifies the difference in hardness observed in the central zone of the deformed footprint of these steels. Compared to its as-received hardness, the decrease in hardness of AISI 12L14 steel is most likely due to lead agglomerations

**Table 4** Wear rate of the discs in the pin-on-disc tests

Cutting speed (m/min)	Steel grade	Stop criterion (min)	Disc weight loss (mg)	Disc wear rate (mg/min)
150	AISI 1018	90	43.83	0.487
	AISI 1212		79.83	0.887
	AISI 12L14		85.41	0.949
180	AISI 1018	70	21.70	0.310
	AISI 1212		58.52	0.836
	AISI 12L14		67.97	0.971
240	AISI 1018	20	6.97	0.348
	AISI 1212		13.52	0.676
	AISI 12L14		20.70	1.035

**Fig. 4** Wear zone, wear tracks and microstructure in pins and discs in AISI 1018 (a), AISI 1212 (b) and AISI 12L14 (c) after reaching the stop criterion in pin-on-disc tests at 150 m/min



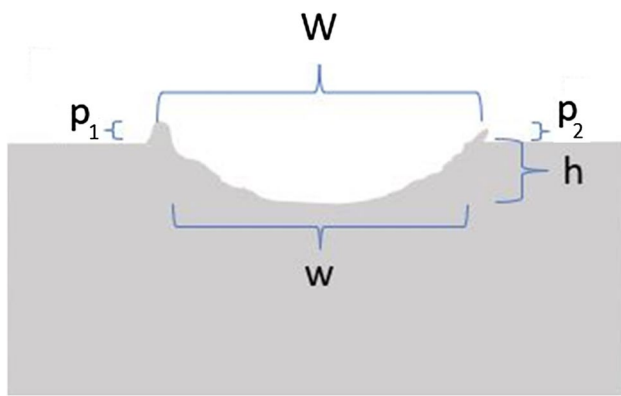


Fig. 5 Profile variables of the wear track

in the deformed zone. The marked asymmetry in disc wear is caused mainly by two reasons. The first is the difference between the material hardness in the plastic deformed zone (see depth Table 5; Fig. 6). Secondly, there is the influence of some chemical components in the microstructure such as manganese sulphides and lead which are in different proportions in each grade of metal studied. For example, AISI 12L14 steel discs present a lower material hardness and higher content of lead. Regarding AISI 1212, the microstructure denotes an important agglomeration of pearlite at the deformed zone (see Fig. 4b), a micro-constituent with higher wear resistance, thus resulting in consistency with wear results found in the experiments for each material [19]. For the remaining steels, the difference could be described by a higher percentage of carbon in AISI 1018 steel than in AISI 1212 (0.247 wt% vs. 0.069 wt%).

### 5 Abrasiveness correlation

Figure 7 illustrates the abrasiveness correlation between wear rates at different cutting speeds and steel grade measured in machining and pin-on-disc tests (see values in Tables 3, 4). Each of the three lines corresponds to a tangential speed (150, 180 and 240 m/min) and on it are gathered wear values obtained by the two methods to be compared (machining and pin on disc) and for a group of low carbon steels sharing a narrow range of initial hardness (HV 0.1 in the range from 171 to 182).

Table 5 Values of the geometrical variable of wear track

Steel grade	W (µm)	w (µm)	h (µm)	p <sub>1</sub> (µm)	p <sub>2</sub> (µm)	Depth (µm)
AISI 1018	1158.3 ± 24.8	959.9 ± 28.1	44.0 ± 6.6	15.8 ± 4.1	22.8 ± 2.5	124.2 ± 18.2
AISI 1212	1915.6 ± 7.5	1524.0 ± 28.7	137.4 ± 6.1	78.8 ± 2.9	88.6 ± 7.9	131.4 ± 19.2
AISI 12L14	1669.2 ± 11.3	1567.7 ± 18.1	125.7 ± 2.7	30.9 ± 3.3	26.2 ± 3.3	82.4 ± 9.2

The regression lines move to the right as speed increases, i.e., the higher the speed, the greater the wear. The linear relationship and its variation with cutting speed make it possible to compare the wear behavior of different low carbon steels and to mutually convert results obtained using the different testing techniques [20]. Based on abrasiveness results, it is possible to design a pin-on-disc test procedure equivalent to a traditional machinability test by considering the following: a) use carbide pins and discs of materials whose machinability is evaluated; b) reproduce cutting speed at the pin-on-disc contact area; c) apply a contact pressure proportional to the ratio between feed force and flank wear area; d) the duration of pin-on-disc test at each cutting speed should be the same as that achieved in machinability test until reaching stop criterion (VB = 0.5 mm), and finally, e) the relative comparison measures are worn rates in mm<sup>3</sup>/min obtained by the two tests.

### 6 Energy cost analysis

The comparative cost analysis between two types of wear tests has been set by taking the most influential five variables. Table 6 corresponds to Argentina's estimated costs as of September 2023.

The comparative cost between these two technologies shows that the pin-on-disc has a lower cost of about 14% compared to the traditional machinability test. Also, note

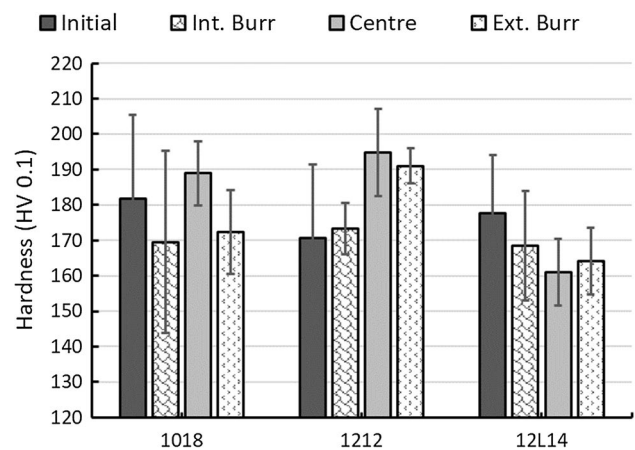
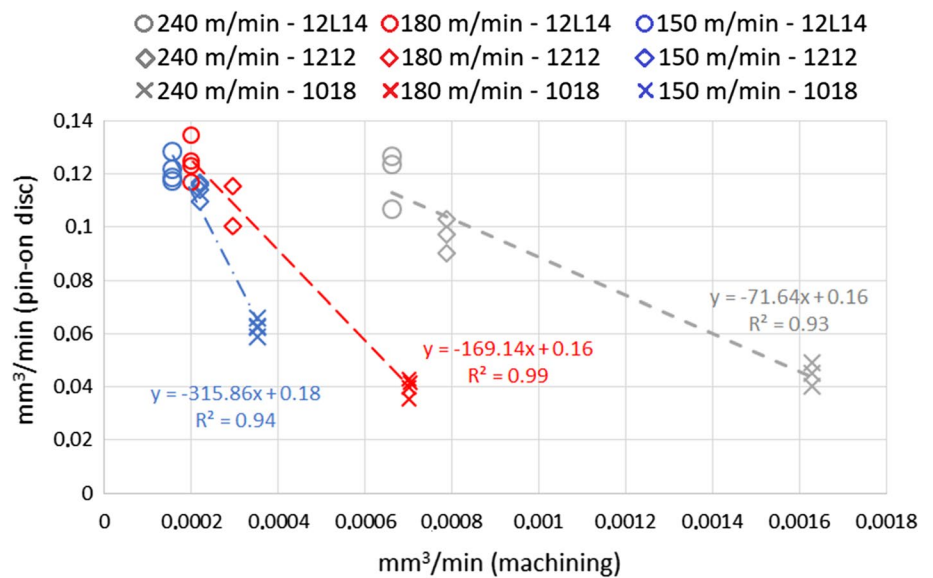


Fig. 6 Material hardness in different zones of the plastically deformed area of discs



**Fig. 7** Wear correlation between the type of wear test, steel grade and cutting speed



**Table 6** Comparative costs for machinability and pin-on-disc tests

Cost	Machining	Pin-on-disc
Materials	1 essay = 120 kg * 6.5 \$US/kg = 780 \$US	1 essay with 4 repetitions = 1 kg = 6.5 \$US
Machine time	9 h = 392 \$US	3.5 h = 10 \$US
Labour	9 h operator + 9 h technician = 662 \$US	3.5 h operator = 204 \$US
Tools	1 cutting insert = 10 \$US	12 pins = 36 \$US
Energy	0.9 kW * 9 h * 0.03 \$US/kW = 0.3 \$US	0.012 kW * 3.5 h * 0.03 \$US/kW ≈ 0 \$US
Total (\$US)	1844.3	256.5

that the energy bill has no critical impact on comparative costs since it is subsidized in Argentina (not in other parts of the world), although the relative energy consumption is 1.3% on pin-on-disc compared with machining. Finally, it is important to emphasize that the costs are seven times lower and the machining time is almost one third when using the pin-on-disc with respect to the usual machining procedure.

## 7 Conclusions

The findings indicate that pin-on-disc tests offer a more efficient and time saving approach to assessing material machinability compared to conventional machining tests. Our study establishes a robust correlation between the traditional machinability test and an equivalent pin-on-disc test across various medium cutting speeds (150–240 m/min) for different carbon steel grades (AISI 1018, AISI 1212 and AISI 12L14). Furthermore, the relative cost-effectiveness of the pin-on-disc test was notable, with a 14% cost compared to the prolonged turning test. Future research will expand this knowledge to encompass alloyed steels, delve deeper into abrasiveness analysis, and explore the broader impact of operational parameters on the processes.

**Acknowledgements** The authors acknowledge Carlos García of Iscar Argentina for providing the carbide pins, Soledad Perera for helping with the EDS analysis of the carbide pins, Mercedes Pianetti for taking the SEM images of the pins and discs and María Emilia Boedo for advising with the spectrography and chemical analysis. Finally, we acknowledge Nora Loureiro for helping analyse the plastically deformed zone.

**Author contributions** All authors contributed to the study conception and design. Daniel Martínez y Antonio Sánchez contributed to conceptualization, methodology, resources, funding acquisition, and writing—review and editing. Vitaliy Martynenko contributed to investigation, validation, visualization, and writing—original draft. Alberto Osenda contributed to methodology, visualization, and writing—review and editing. All authors read and approved the final manuscript.

**Funding** Open Access funding provided thanks to the CRUE-CSIC agreement with Springer Nature. Antonio Sánchez is supported by the Serra Hünter program (Generalitat de Catalunya).

## Declarations

**Conflict of interest** The authors declare no competing interests.

**Open Access** This article is licensed under a Creative Commons Attribution 4.0 International License, which permits use, sharing, adaptation, distribution and reproduction in any medium or format, as long as you give appropriate credit to the original author(s) and the source, provide a link to the Creative Commons licence, and indicate if changes



were made. The images or other third party material in this article are included in the article's Creative Commons licence, unless indicated otherwise in a credit line to the material. If material is not included in the article's Creative Commons licence and your intended use is not permitted by statutory regulation or exceeds the permitted use, you will need to obtain permission directly from the copyright holder. To view a copy of this licence, visit <http://creativecommons.org/licenses/by/4.0/>.

## References

1. Pervaiz S, Kannan S, Kishawy H (2018) An extensive review of the water consumption and cutting fluid based sustainability concerns in the metal cutting sector. *J Clean Product* 197(1):134–153. <https://doi.org/10.1016/j.jclepro.2018.06.190>
2. Naskar A, Chattopadhyay A (2018) Investigation on flank wear mechanism of CVD and PVD hard coatings in high speed dry turning of low and high carbon steel. *Wear* 396–398:98–106. <https://doi.org/10.1016/j.wear.2017.11.010>
3. Chinchani S, Choudhury S (2015) Machining of hardened steel: experimental investigations, performance modeling and cooling techniques: a review. *Int J Mach Tools Manuf* 89:95–109. <https://doi.org/10.1016/j.ijmactools.2014.11.002>
4. Luiz N, Machado A (2008) Development trends and review of free-machining steels. *Proc Inst Mech Eng Part B* 222(2):347–360. <https://doi.org/10.1243/09544054JEM861>
5. Essel I (2006) Machinability enhancement of non-lead Free-cutting Steel. , Doctoral thesis, Shaker Verlag. ISBN: 9783832253103
6. Singh Gill S, Singh H, Singh R, Singh J (2011) Flank wear and machining performance of cryogenically treated tungsten carbide inserts. *Mater Manuf Process* 26(11):1430–1441. <https://doi.org/10.1080/10426914.2011.557128>
7. ISO 3685:1993(E) International Standard (1993) Tool testing with single point turning tools. International Organization for Standardization, Geneva
8. Salak A, Vasilko K, Selecka M, Danninger H (2006) New short time face turning method for testing the machinability of PM steels. *J Mater Process Technol* 176:62–69. <https://doi.org/10.1016/j.jmatprotec.2006.02.014>
9. Standard UNE 36423:1990. Tests on steels. Machinability index determination. Turning methods by short time tool-life testing
10. Ståhl JE, Andersson M (2007) Polar machinability diagrams—a model to predict the machinability of a work material. In: Swedish production symposium, Göteborg, Sweden
11. Xu L, Schultheiss F, Andersson M, Ståhl J (2013) General conception of polar diagrams for the evaluation of the potential machinability of workpiece materials. *Int J Mach Mach Mater* 14(1):24–44. <https://doi.org/10.1504/ijmmm.2013.055119>
12. Kümmel J, Gibmeier J, Schulze V, Wanner A (2014) Effect of built-up edge formation on residual stresses induced by dry cutting of normalized steel. *Adv Mater Res* 996:603–608. <https://doi.org/10.4028/www.scientific.net/AMR.996.603>
13. Avdovic P, Xu L, Andersson M, Stahl J (2011) Evaluating the machinability of inconel 718 using polar diagrams. *J Eng Gas Turbines Power* 133:7. <https://doi.org/10.1115/1.4002679>
14. Martínez Kraemer D, Hameed S, Sánchez Egea AJ, Pérez D, Canales J, López de Lacalle LN (2019) Wear and MnS layer adhesion in uncoated cutting tools when dry and wet turning free-cutting steels. *Metals* 9:556. <https://doi.org/10.3390/met9050556>
15. Martínez Kraemer D, Urbicain G, Sánchez Egea A (2020) Dry machinability analyses between free cutting, resulfurized, and carbon steels. *Mater Manuf Process*. <https://doi.org/10.1080/10426914.2020.1734615>
16. Machinability Data Center (1980) Machining data handbook, vol 1. MDC. ISBN 9780936974019. <https://books.google.es/books?id=bKKuzgEACAAJ>
17. Xu J, An Q, Chen M (2012) Experimental study on high-speed turning of free-cutting steel AISI 408 12L14 using multi-layer coated carbide tools. *Adv Mater Res* 500:3–7. <https://doi.org/10.4028/www.scientific.net/AMR.500.3>
18. Pervaiz S, Rashid A, Deiab I, Nicolescu M (2014) Influence of tool materials on machinability of titanium- and nickel-based alloys: a review. *Mater Manuf Process* 29(3):219–252. <https://doi.org/10.1080/10426914.2014.880460>
19. Hernández-Sierra MT, Aguilera-Camacho LD, Báez-García JE, García-Miranda JS, Moreno KJ (2018) Thermal stability and lubrication properties of biodegradable castor oil on AISI 4140 steel. *Metals* 8:428. <https://doi.org/10.3390/met8060428>
20. Fu L, Li L (2013) Li D (2013) Further look at correlation between ASTM G65 rubber wheel abrasion and pin-on-disc wear tests for data conversion. *Tribol Mater Surf Interfaces* 7(3):109–113. <https://doi.org/10.1179/1751584X13Y.0000000031>

**Publisher's Note** Springer Nature remains neutral with regard to jurisdictional claims in published maps and institutional affiliations.